19. Slip Bands, Twins, and Precipitation Processes in Fatigue Stressing

M. R. HEMPEL

Max-Planck-Institut für Eisenforschung
Düsseldorf, Germany

ABSTRACT

This chapter contains the results of investigations on the deformation phenomena and structural changes occurring in materials under alternating stress and at different test conditions. These investigations comprised a study of the formation of slip lines appearing in metallic materials at room temperature, as well as of the formation of twins at low temperatures and the occurrence of precipitation processes at high temperatures.

Introduction

In the course of repeated loading of a material, three ranges are generally to be considered (Fig. 1). In Range I, no failures will occur, but changes in the properties and structure of the material are possible. Range II is the range of overstressing in which the appearance of greater changes in the properties and of microcracks in the structure will be possible. Range III embraces the damage zone in which macrocracks and fatigue failures are to be expected.[1]

A prerequisite to the establishment of a theory of the fatigue limit [2–4] is knowledge of the processes that lead to property changes and structural changes. For several years, a series of investigations has been carried out in the Max Planck Institute for Iron Research at Düsseldorf to determine the deformation phenomena and structural changes occurring in cyclically stressed materials. In the following pages, a report will be given on the formation of slip traces, the propagation of cracks at room temperature, the formation of twins at low temperatures, and the precipitation of carbides in steels at elevated temperatures.

Formation of Slip Lines at Room Temperature

When metallic materials are stressed alternately, plastic deformation processes occur in the same way as in the static test. These deformation processes are called slip,[5–7] and they are attributed to the formation and movement of dislocations.[8–12] Within the scope of a larger program to investigate the deformation phenomena occurring under cyclic stress at

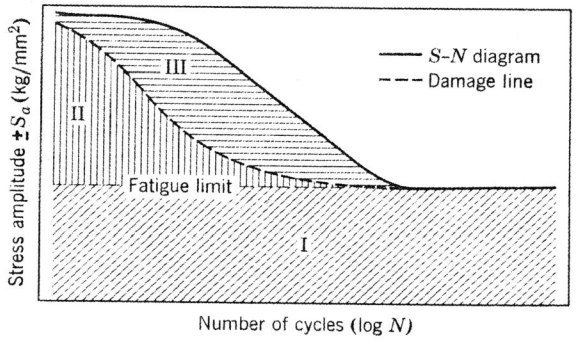

Fig. 1. Fatigue diagram. I = region of unlimited lifetime; II = range of overstressing; III = range of overstressing with damage and fracture.

room temperature, tests have been carried out on polycrystalline and single-crystal specimens of body-centered cubic materials, as well as on polycrystalline face-centered cubic materials. In order to determine the effect of stress concentrations on the formation and propagation of slip traces, flat specimens, either with a transverse hole 2 mm in diameter or with edge V-notches (60°, depth = 1.5 mm, root radius = 0.1 mm), have been used, in addition to unnotched flat specimens. Before starting with reversed bending fatigue tests (at 1500 cpm with $S_m = 0$), the surfaces of ground specimens were mechanically or electrolytically polished and then etched. They were not usually subjected to any further treatment during a test. The slip traces were examined with bright-field illumination or by means of the phase-contrast method in the light microscope, as well as by means of plastic replicas in the electron microscope.

Polycrystalline Specimens of a Body-Centered Cubic Material

The influence of stress on the slip processes has been examined on an unalloyed steel.* [13–15] A typical example is given in Fig. 2 of the forma-

* Steel with 0.09% C, 0.01% Si, 0.62% Mn, 0.041% P, 0.023% S, 0.009% N, and 0.02% O; yield strength = 24.8 kg/mm²; ultimate tensile strength = 39.6 kg/mm².

tion and propagation of the slip traces on identical areas of the surface of an unnotched specimen stressed below the fatigue limit. Slip traces appear in only those few crystallites that are favorably oriented with respect to the direction of the load. Up to 46×10^6 reversals of stress, the number and extent of the slip lines steadily increase.

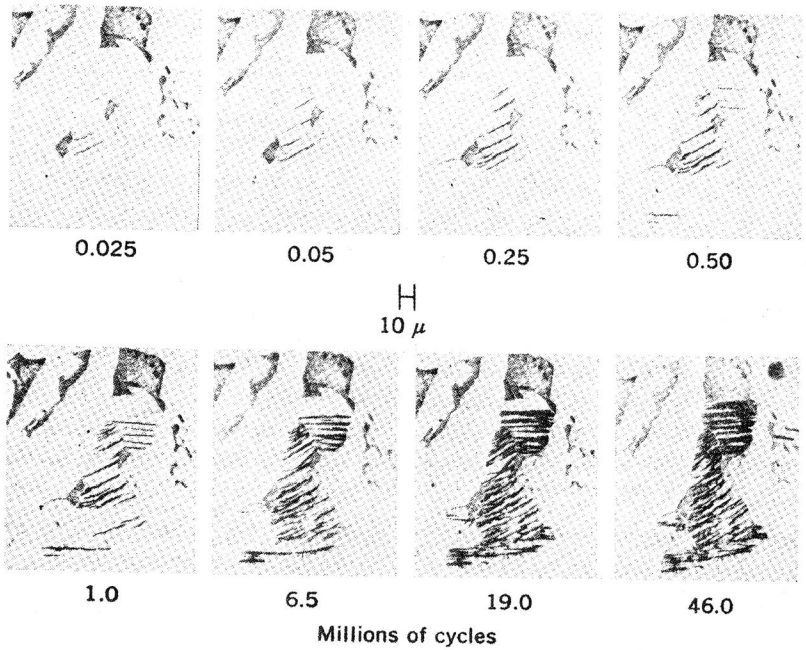

Fig. 2. Formation of slip bands in 0.09% C steel at a stress below the fatigue limit. Plane-bending fatigue test. Mean stress $S_m = 0$, stress amplitude $S_a = \pm 17.5$ kg/mm², 1500 cpm.

The moment of the formation of the first slip lines and the rate of their propagation depend largely on the level of stress. Figure 3 shows the S–N diagram for unnotched specimens, as well as the line indicating the appearance of the first slip traces at the various stress amplitudes. At loads above the fatigue limit, the first slip lines can be seen after a few thousand cycles; with decreasing stress, their appearance is displaced to higher numbers of reversals. Figure 4 shows the effect of the stress level on the formation of the slip traces after 0.25×10^6 cycles. A stress amplitude of ± 14.0 kg/mm² (20,000 psi), being about 22% below the fatigue limit, does not lead to formation of any slip lines even after a number of cycles reaching 15×10^6. With stress amplitudes of ± 16.0 and ± 17.5 kg/mm² (just below the fatigue limit), slip traces appear only

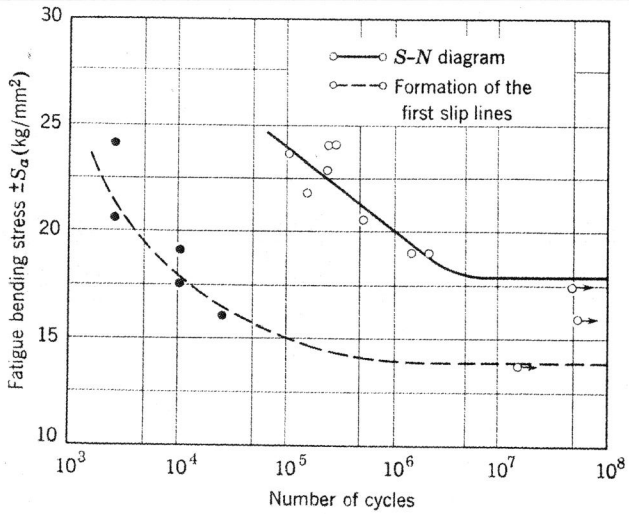

Fig. 3. Occurrence of the first slip lines on unnotched flat specimens of 0.09% C steel.

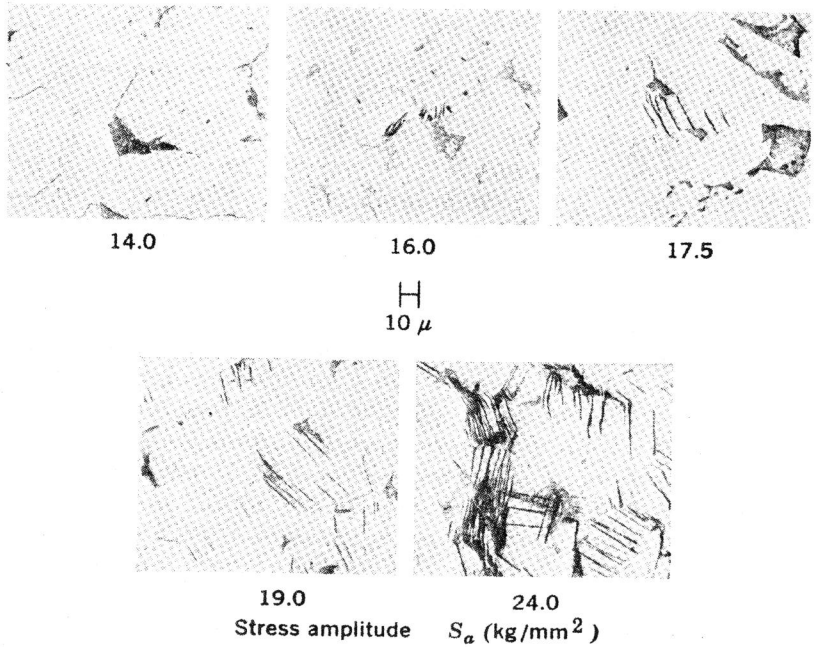

Fig. 4. Formation of slip bands dependent on the stress $\pm S_a$. 0.25×10^6 cycles.

in individual crystallites. With stresses of ±19.0 and ±24.0 kg/mm² (above the fatigue limit), slip traces are more distinct and are present in numerous crystallites.

As regards formation and propagation, the slip traces found in notched specimens differ in no way from those observed in unnotched bars.[16] The slip traces are confined to the immediate vicinity of the root of the

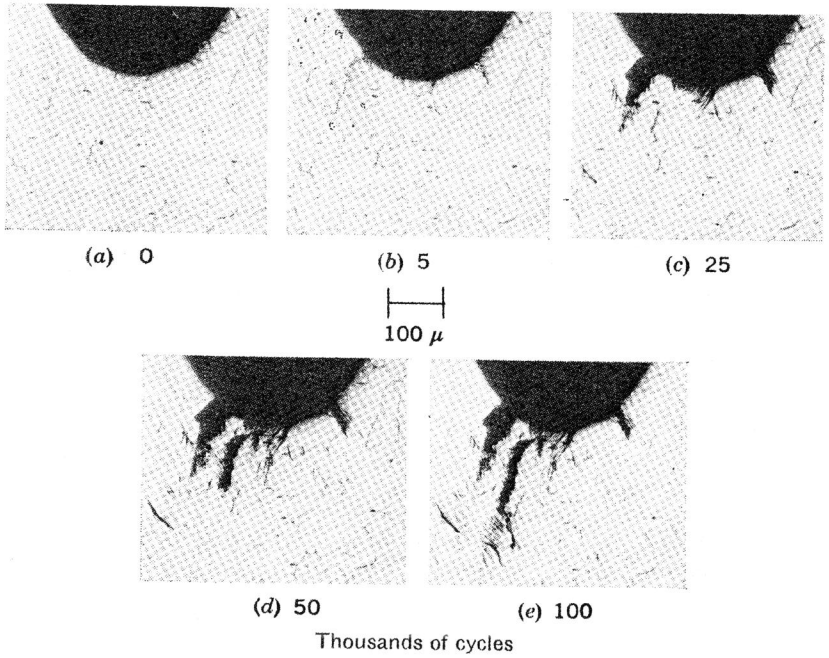

Fig. 5. Slip bands on 0.09% C steel specimen with V-shaped notch. $S_a = \pm 14.0$ kg/mm².

notch and occur at lower stresses because of the stress concentration at the notch. Figure 5 shows as an example the formation of the slip traces on a V-notched specimen. Here the first slip traces can be observed after a test duration of only 0.02% of the total lifetime. From Figs. 5*b* and 5*c*, it may be observed that the deformation traces appear in progressively larger zones of the notch root. It is only after test durations of 50,000 to 100,000 cycles (Figs. 5*d* and 5*e*) that slip occurs in the crystallites that are in the immediate neighborhood of the stress peak.

In order to examine whether the slip band contains real fissures, and if so, when they first appear, use is made in many cases of the method of repeated polishing and etching of the surface after different steps of load. Results of such an experimental procedure are given in Fig. 6 for a bar

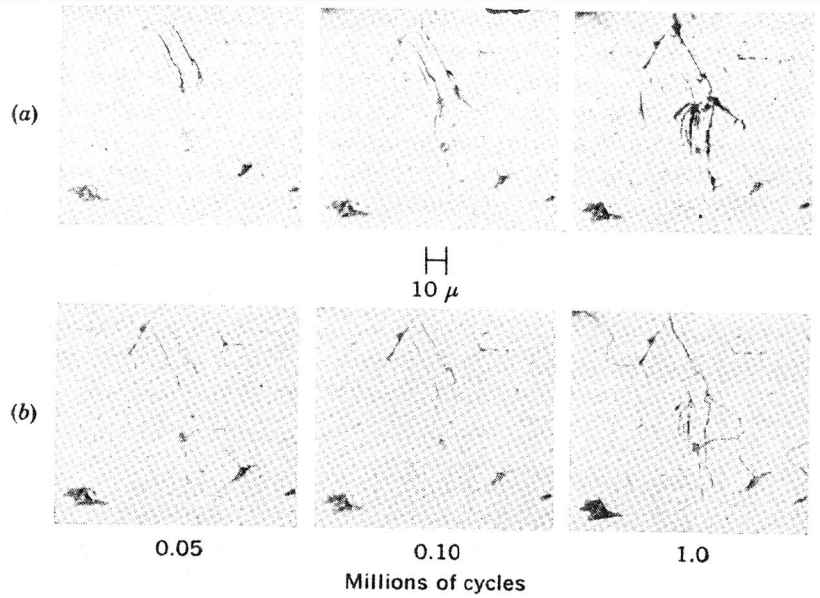

Fig. 6. Appearance of slip bands in 0.09% C steel after cyclic stressing, repolishing, and etching. Flat specimen with a transverse hole. $S_a = \pm 14.0$ kg/mm². (*a*) After cyclic stressing. (*b*) After repolishing and etching.

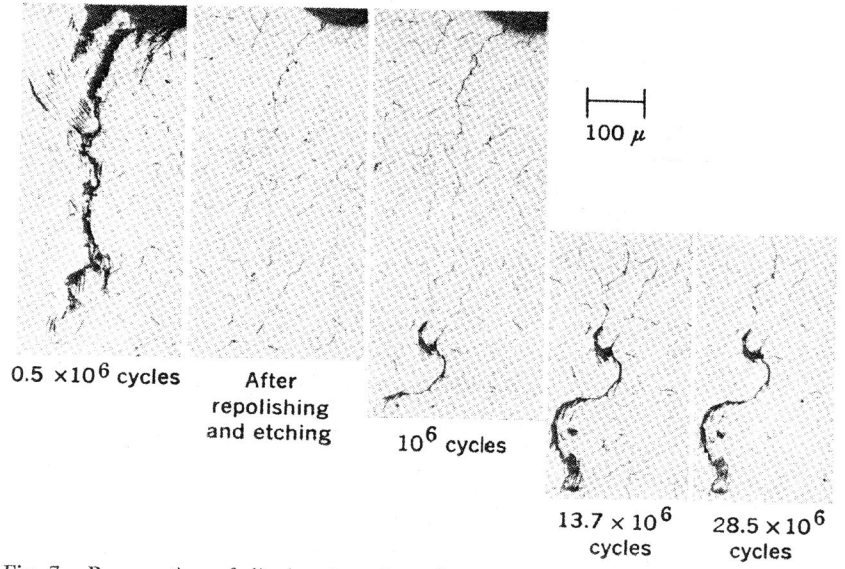

Fig. 7. Propagation of slip bands and cracks on notched specimen, 0.09% C steel. V-shaped notch.

with a transverse hole.[14] The photographs distinctly show that, upon repolishing, those slip bands disappear that contain no microcracks (or only extremely flat ones) and that only the slip bands interspersed with deep microcracks remain visible as fine crack lines. It can be recognized, furthermore, that new slip traces in the load steps to follow will be substantially confined to those crystallites that are not yet cracked.

Figure 7 shows that it is not feasible to conclude from the appearance of slip traces and microcracks that, in every case, they will lead to the formation of macrocracks and fatigue failure. This collection of photographs represents the continuation of the tests carried out on the specimen shown in Fig. 5. After 0.5×10^6 cycles, the specimen was repolished and etched and then tested at the same stress to 1.0, 13.7, and 28.5×10^6 cycles. The following sequence of results is obtained:

1. After 0.5×10^6 cycles, repolishing and etching remove the slip traces, and the crack line is distinctly outlined.

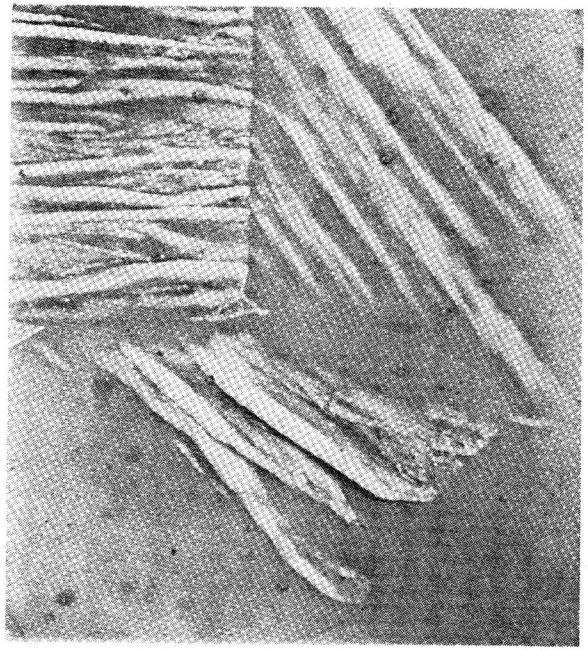

Fig. 8. Slip markings in adjacent crystals. Unnotched 0.09% C steel specimen. $S_a = \pm 17.5$ kg/mm², 19×10^6 cycles.

2. After 10^6 cycles, the slip lines appear again, but only at the end of the crack line.
3. After 13.7×10^6 cycles, the area of slip lines increases very little.
4. After 28.5×10^6 cycles, the slip traces stop propagating.

These findings confirm the observations made by Frost and Phillips [17] on nonpropagating cracks.

For examination of further details of the structure of individual slip bands, the light microscope is inadequate, while the electron microscope is particularly suitable. Figure 8 shows the development of slip bands in adjacent crystals. The slip bands mostly appear as straight, well-arched, slip lamellae standing out from the undeformed portion of the ferrite grains. The directions of the lamellae in the three grains are dif-

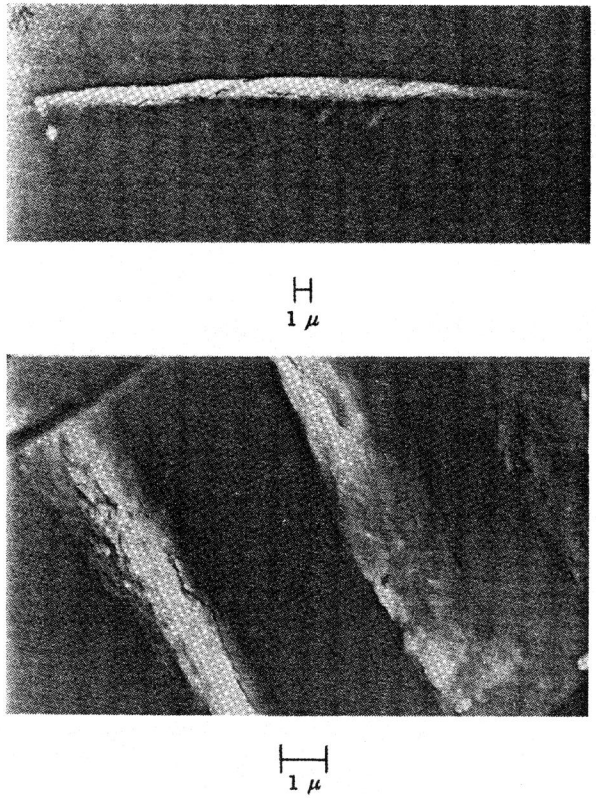

Fig. 9. Cracks on the surface of slip bands (plastic replica). Unnotched 0.09% C steel specimen. $S_a = \pm 19.0$ kg/mm², 1.56×10^6 cycles.

ferent, from which it may be inferred that these grains have different orientations. Figure 9 shows the surface appearance of some slip bands that have formed in a specimen stressed just above the fatigue limit. Here the undeformed ferrite seems to be dark shaded, and the light-shaded slip bands seem to arch out from the ferrite. The slip bands have a pitted surface showing numerous fine dark lines and some crevicelike grooves and splits. Electron micrographs of slip bands in ferritic materials show quite distinctly that, in the course of fatigue stressing, submicroscopic cracks develop at the surface of individual slip bands. Given an added amount of vibration energy, these fine fissures join to form microcracks or macrocracks which then lead to fatigue failure.

Single-Crystal Specimens of a Body-Centered Cubic Material

To investigate further the deformation phenomena accompanying cyclic stressing, fatigue tests have been carried out on α-iron single crystals, with the aim of determining the influence of crystal orientation on the fatigue limit and on the formation of slip traces.[18–20] For the purpose of

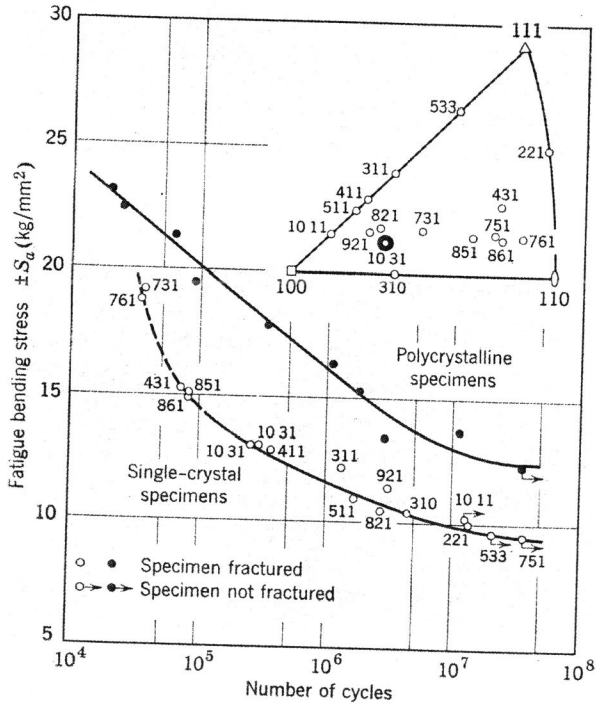

Fig. 10. S–N diagram of single-crystal and polycrystalline specimens of α-iron with a carbon content of 0.006%.

these studies, single crystals of Armco iron with 0.006% C were made by the strain-anneal technique, and their orientations were determined by back-reflection Laue diagrams. Figure 10 represents the S–N diagram of the differently oriented single-crystal specimens. The figures entered at the test points indicate the crystallographic direction of the nominal bending stress (x-direction = direction of the longitudinal axis of the bar). The x-directions are also indicated on the stereographic triangle in Fig. 10. The test points fall with relatively small scatter on a mean S–N line, showing that the different orientations of the specimens affect their lifetime to only a small extent. This finding is easy to understand, since the specimens tested have orientation factors $\mu = \tau/\sigma_N$ (τ = shear stress, σ_N = nominal stress) that differ but little from the maximum value of 0.5.

Using the light and electron microscopes, additional studies have been carried out on the cyclic-stressed single-crystal specimens. These investigations were intended to find the effect of crystal orientation and stress conditions on the formation of slip lines. Figure 11 shows photographs

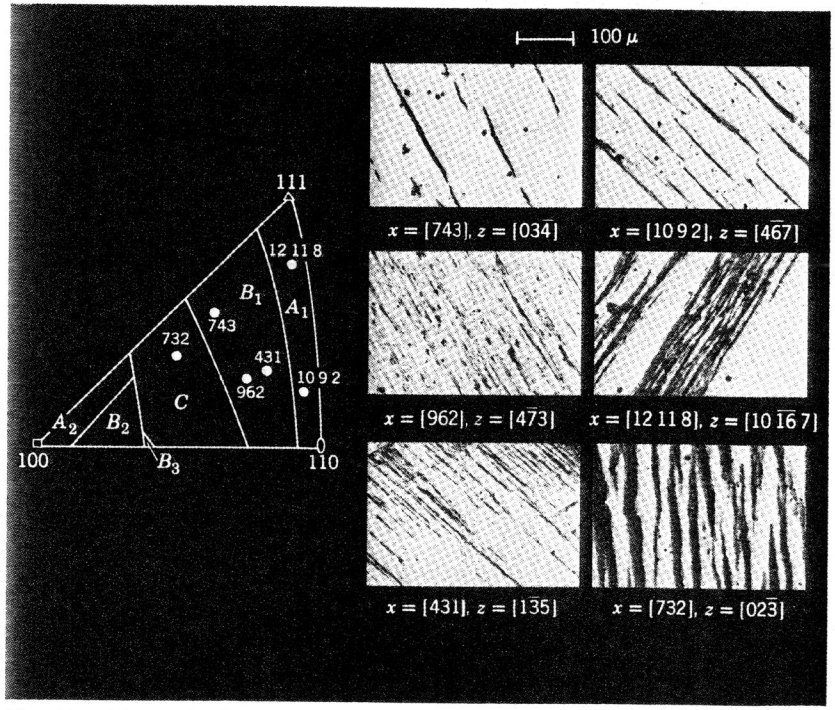

Fig. 11. Slip markings at the surface of cyclically stressed single-crystal specimens with orientations lying in the middle parts of the orientation ranges (single slip).

of slip lines of some fatigued single crystals in which the crystallographic directions of the bending stresses (x-direction) fall in the middle of one of the possible slip-system orientation ranges, A, B, or C,[21] for α-iron. Stress level and number of reversals, both of which affect the appearance of the slip markings considerably, vary widely from specimen to specimen. In spite of this, single slip occurs in each case, leading to the formation of long, straight slip lines.

If the crystallographic orientations are not situated in the central portion of one of the slip system ranges (A, B, or C) but are near the border line of two orientation ranges, the simultaneous operation of the slip systems adjoining this border line leads to multiple slip with small plastic deformation. Figure 12 shows the effect of multiple slip on the appearance of the slip traces in the case of some border-line oriented single-crystal specimens. Multiple slip is responsible for the appearance of the wavy slip lines.

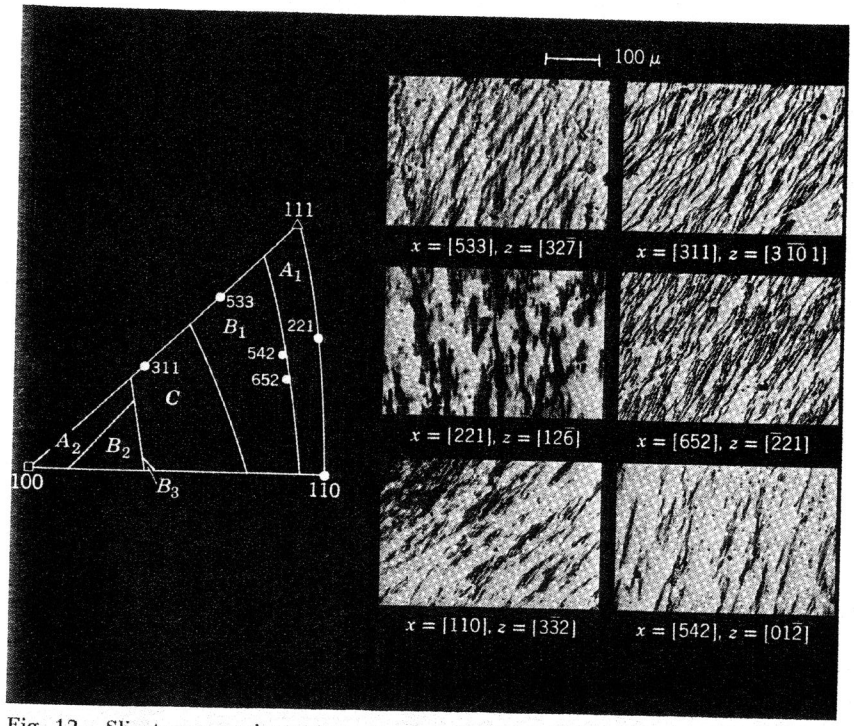

Fig. 12. Slip traces at the surface of cyclically stressed single-crystal specimens with orientations lying near the border lines of the different orientation ranges (multiple slip).

Electron micrographs of slip bands in a border-line-oriented specimen are presented in Fig. 13. The wavy course of the individual slip bands proves to be an accumulation of several slip lamellae that were arched out from the ferrite to a different extent (Fig. 13, top). In the highly

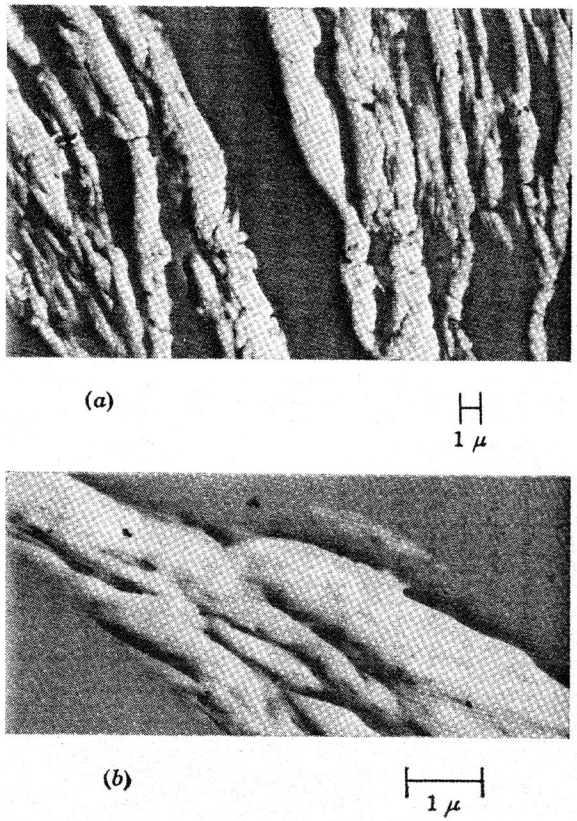

Fig. 13. Electron micrograph (plastic replica) of slip bands in α-iron single-crystal specimen oriented for multiple slip. x = [311], z = [3$\bar{1}\bar{0}$1]; S_a = ±15.5 kg/mm²; 4.003 × 10⁶ cycles (to fracture).

stressed portion of the test specimen, the slip bands attain a width of up to 15 μ (Fig. 13, bottom); they show heavy deformation in which numerous fissures are to be seen.

In order to relate these studies to those made on the polycrystalline specimens, the effect of the grain boundaries on the deformation phenomena has been examined in bicrystal and tricrystal bars. The left-

hand and central parts of Fig. 14 show the influence of test duration on the formation of slip markings in bicrystal specimens in which the grain boundary is situated nearly perpendicular or parallel to the stress direction. The right-hand part of Fig. 14 refers to the same influence on a

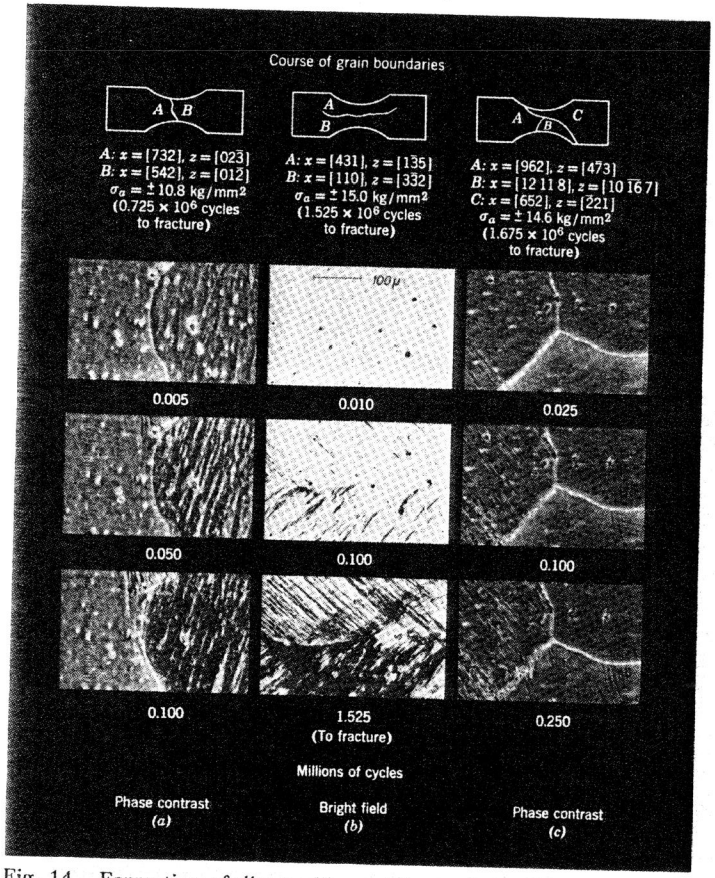

Fig. 14. Formation of slip markings at the surface of bicrystalline and tricrystalline specimens of α-iron.

tricrystal specimen. Slip lines are seen to form after different numbers of cycles in differently oriented crystals, and an effect of inclusions is also apparent. The pattern of slip bands and fatigue cracks in these multicrystal bars is shown by the photographs in Fig. 15. In the left-hand specimen, the fatigue failure runs dominantly along the grain boundary and perpendicular to the direction of the bending stress. Only a narrow zone of slip markings develops, and that is located near the

grain boundary. In the bicrystal specimen with the boundary parallel to the direction of the bending stress, stronger slip traces occur over a larger area. In addition to the actual fatigue failure, other cracks are present which start from the grain boundary as well as from the edge of

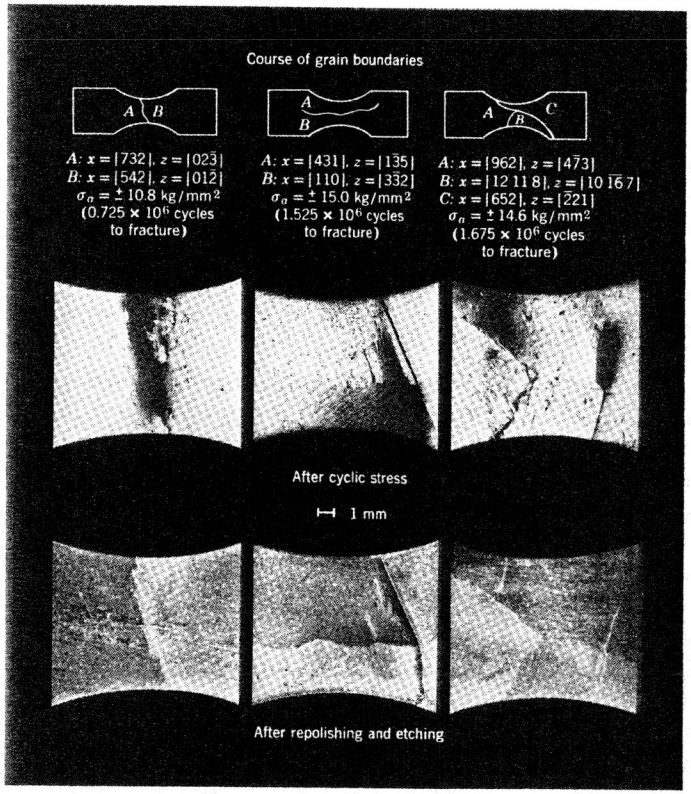

Fig. 15. Range of slip traces and course of cracks in bicrystalline and tricrystalline specimens of α-iron.

the specimen. The very different formation of slip markings in the tricrystal bar is shown in the right-hand part of Fig. 15. There are numerous cracks in the individual grains, many of which start within the grain boundaries. This leads to the supposition that the distortions occurring at boundaries favor the initiation of a fatigue failure.

The investigations carried out on the single crystals of α-iron show clearly that the slip mechanism in fatigue stressing is the same as that in static tension. The same slip systems are active, $<111>\{112\}$, $<111>\{123\}$, and $<111>\{110\}$, and at the same time these planes are the directions of

the fatigue cracks occurring in the ferrite. Attention should be paid to the fact that the initiation of the first cracks may proceed at different places in the test section: (1) In single-crystal and polycrystalline specimens, they start at the surface of the slip bands; (2) in multicrystal bars, they start at the grain boundaries, which, because of the anisotropic behavior of the adjoining crystals, will be severely deformed; or (3) they may start at nonmetallic inclusions because of the stress concentration occurring there.

Polycrystalline Specimens of Face-Centered Cubic Materials

In order to investigate the effect of stress on the deformation phenomena in face-centered cubic metals, bending fatigue tests were carried out on unnotched flat specimens of pure aluminum, two aluminum alloys, and two austenitic steels.

Pure aluminum. Specimens of 99.99% aluminum were annealed ½ hr at 350°C* and then electrolytically polished. The endurance limit was about ±1.5 kg/mm² (10^8 cycles) and agreed approximately with the value of the static yield strength.[22] The number and extent of the deformation markings are affected, above all, by the stress amplitude and by the test duration. Figure 16 shows an example of the effect of stress on the formation of the slip traces at 0.25×10^6 cycles. The slip markings appear as regularly arranged lines in certain areas of different crystallites. They grow longer and wider with an increasing number of cycles, and new slip bands form in the same or in other crystallites. At a stress corresponding approximately to half the value of the endurance limit, slip lines appear at only a few places in individual crystallites (Fig. 16*a*). A stress of approximately 60% of the value of the endurance limit already leads to wide slip traces in individual crystallites; the number and extent of the slip bands increase considerably at stresses close below and above the fatigue limit (Figs. 16*c* and *d*). Slip lines in aluminum also vary greatly in appearance, depending on whether the slip is single or multiple (Fig. 17). Figure 18 shows two electron micrographs of the formation of slip lines near a grain boundary. The dark spots in the micrographs indicate cavities in the surface. These spots and the slip bands have also been examined by using Al_2O_3 film replicas. In Fig. 19*a*, three grains with slip markings are shown. The oxide film is observed from the interior of the bar, that is, from the side of the removed aluminum. The dark spots represent cavities that now and then occur in rows, extending to a considerable depth below the surface. This is confirmed by the investigation of test samples cut perpendicular to the surfaces (Fig. 19*b*).

* Stress for a permanent set of 0.2% = 1.33 kg/mm², ultimate tensile strength = 5.13 kg/mm².

The surfaces of the specimen show a wavy shape and numerous grooves with bag- or hole-shaped enlargements extending to a depth of about 0.02 mm. These holes become visible if the surface is cautiously removed by polishing (Fig. 20). After a layer of 5-μ thickness is polished away,

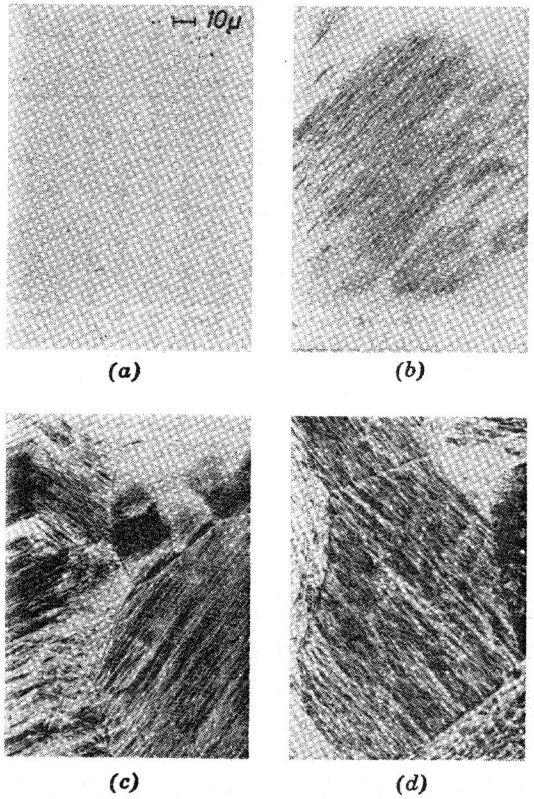

Fig. 16. Effect of increasing stress level on the appearance of slip markings in pure aluminum at a constant number of cycles, 0.25×10^6. S_a = (*a*) ±0.73 kg/mm², (*b*) ±0.93 kg/mm², (*c*) ±1.34 kg/mm², (*d*) ±1.74 kg/mm².

whole fields with holes appear in many grains (Fig. 20*a*). With further polishing, the holes and pit areas become more rare, but they are still evident at a depth of about 11 μ (Fig. 20*b*). The formation of such cavities can be expected theoretically. It is the result of a piling-up of vacancies that form during the movement of dislocations.[23]

Aluminum alloys. In order to examine the way in which the structure of heat-treated aluminum alloys affects the formation of deformation

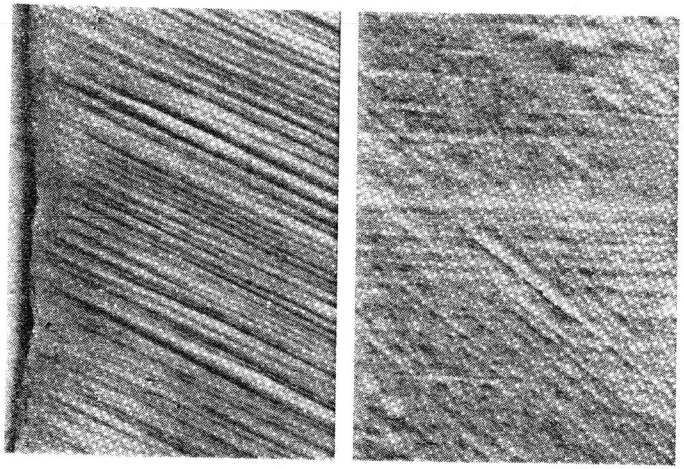

Fig. 17. Electron micrographs (plastic replica) of deformation lines in cyclically stressed specimens of pure aluminum oriented for single and multiple slip. $S_a = \pm 1.0$ kg/mm². (*a*) 15×10^6 cycles. (*b*) 30×10^6 cycles.

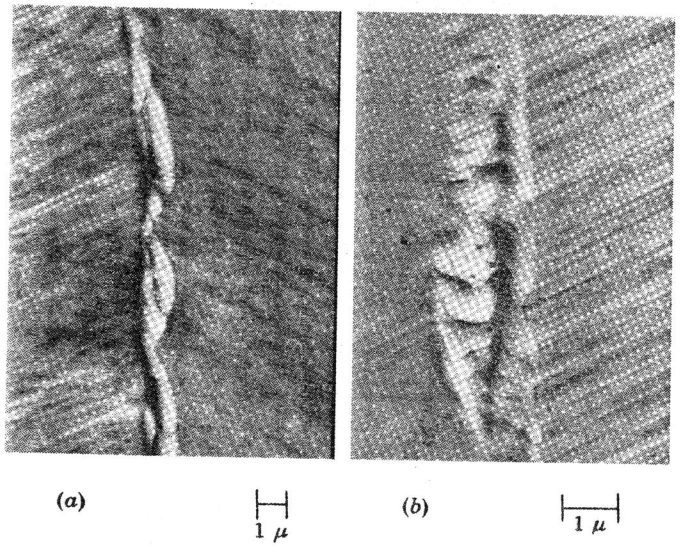

Fig. 18. Electron micrographs (plastic replica) of slip markings in pure aluminum near grain boundaries. $S_a = \pm 1.0$ kg/mm², 15×10^6 cycles.

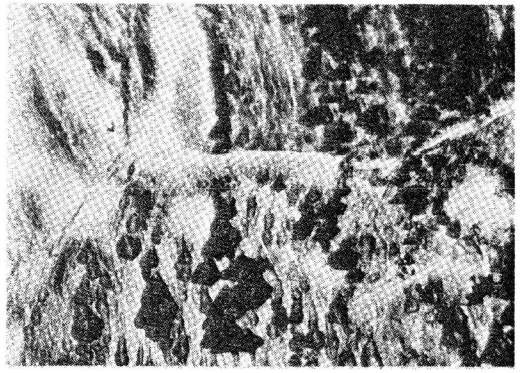

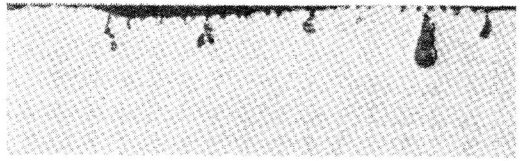

Fig. 19. (*a*) Electron micrograph (Al_2O_3 film replica) of surface of cyclically stressed aluminum specimen. (*b*) Light micrograph of transverse section, unetched. $S_a = \pm 1.74$ kg/mm², 1.75×10^6 cycles (to fracture).

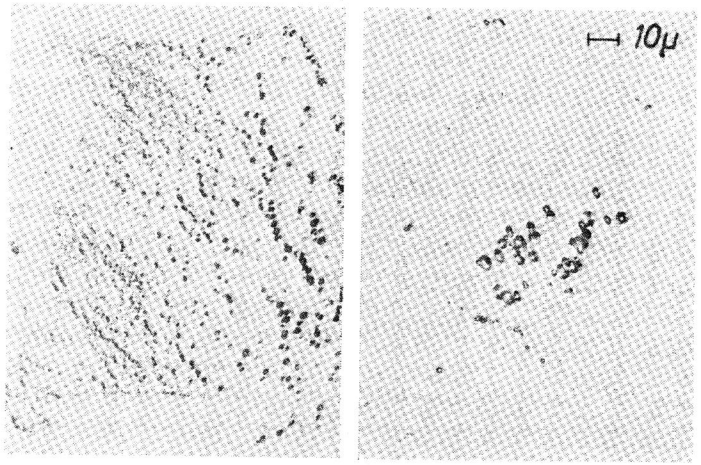

Fig. 20. Surface appearance of a fatigued specimen (unetched) after polishing in several steps parallel to the surface (see Fig. 19*a*). (*a*) 5 μ below the surface. (*b*) 11 μ below the surface.

markings, the investigations were extended to one aluminum alloy each of the type Al-Mg-Si and one of the type Al-Zn-Mg-Cu.[16] The chemical composition, heat-treatment, and strength of these materials are given in Table 1. The structure of these materials is characterized by inclusions of the alloying constituents in an irregular arrangement or in lines.

TABLE 1. Chemical Composition, Heat-Treatment, and Strength Values of Two Aluminum Alloys

	Al-Mg-Si	Al-Zn-Mg-Cu
Chemical Composition (%)		
Mg	0.77	2.80
Si	0.82	0.24
Zn	—	5.95
Cu	0.045	1.72
Mn	0.63	0.19
Fe	0.31	0.29
Cr	—	0.15
Ti	0.014	0.011
Heat-Treatment	15 min at 530°C, water-quenched; age-hardened 16 hr at 150°C	15 min at 475°C, water-quenched; age-hardened 20 hr at 120°C
Yield Strength (kg/mm²)	27.7	49.4
Ultimate Tensile Strength (kg/mm²)	32.5	57.9
Fatigue Limit * (kg/mm²)	±11.0	±14.0

* Reversed plane-bending fatigue test: $S_m = 0$, 1500 cpm, 10^8 cycles.

The first slip lines in these materials could be made evident in the light microscope only with the aid of the phase-contrast method. Figure 21 contains an example of the Al-Mg-Si alloy. It should be particularly noted that the slip lines appearing after 2500 cycles change little up to 50,000 cycles. On the other hand, cracking takes place immediately after the beginning of the test, particularly at inclusions, and proceeds steadily (arrows in Fig. 21). The different formation of deformation markings in the Al-Zn-Mg-Cu alloy can be seen in Fig. 22. Here, the slip lines run mostly in a straight line, but they are frequently interrupted and show the cross slip typical of face-centered cubic materials.[24] In Fig. 23 are some examples which show that, even with the bright-field illumination of the light microscope, slip traces can be discerned in the Al-Mg-Si alloy only in connection with cracks having appeared simultaneously.

The reason that there is cracking simultaneous with the occurrence of slip lines in these aluminum alloys is due to the low strain hardenability of these materials, as well as the notch effect present at the numerous in-

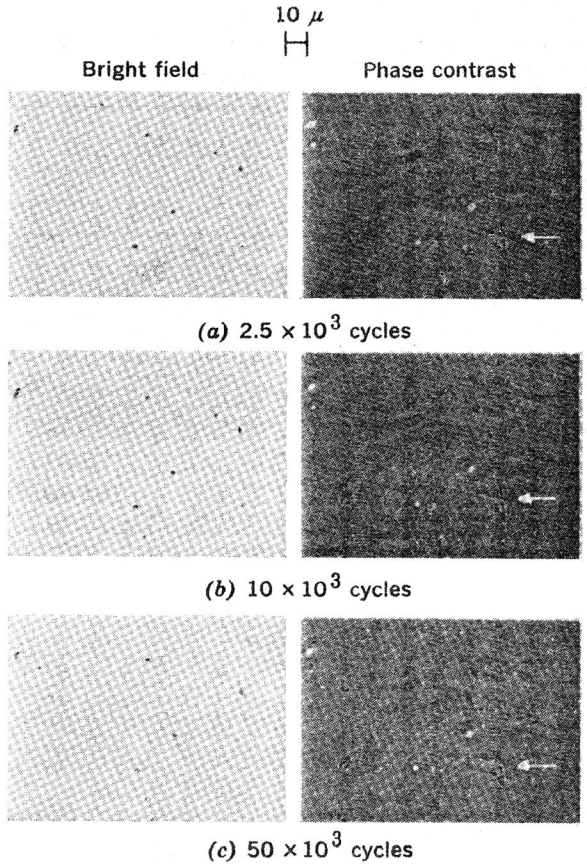

Fig. 21. Effect of number of cycles on the formation of slip traces in a flat specimen of Al-Mg-Si alloy. S_a = ±21.7 kg/mm². 0.258 × 10^6 cycles to fracture.

clusions. The photographs in Fig. 24 show distinctly the cracking at the inclusions, as well as the course of the cracks running from one inclusion to another.

Austenitic steels. Two austenitic steels have been tested.[16] One of these corresponds to Type 17 Mn; the other to Type 15 Cr-15 Ni, to which have been added the further alloying elements of Mo, Cb, and N.

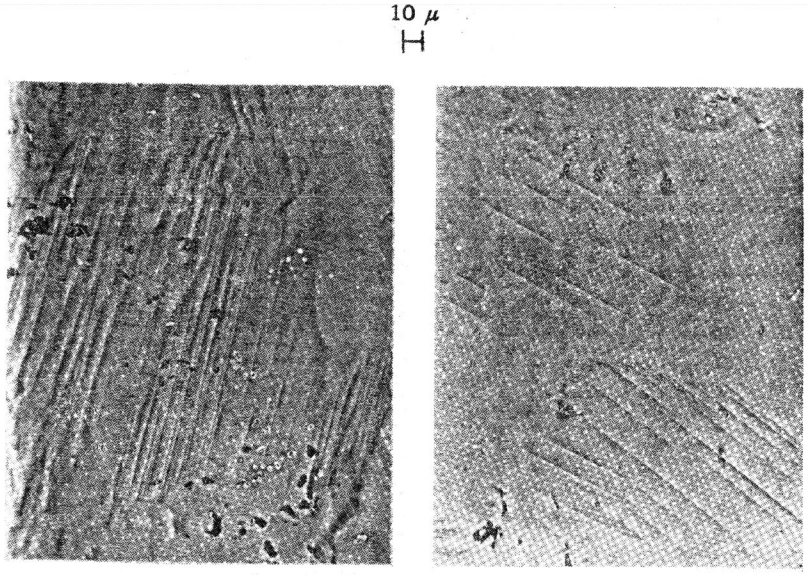

Fig. 22. Slip markings in a flat specimen of Al-Zn-Mg-Cu alloy (phase-contrast method). $S_a = \pm 25.0$ kg/mm², 0.2×10^6 cycles.

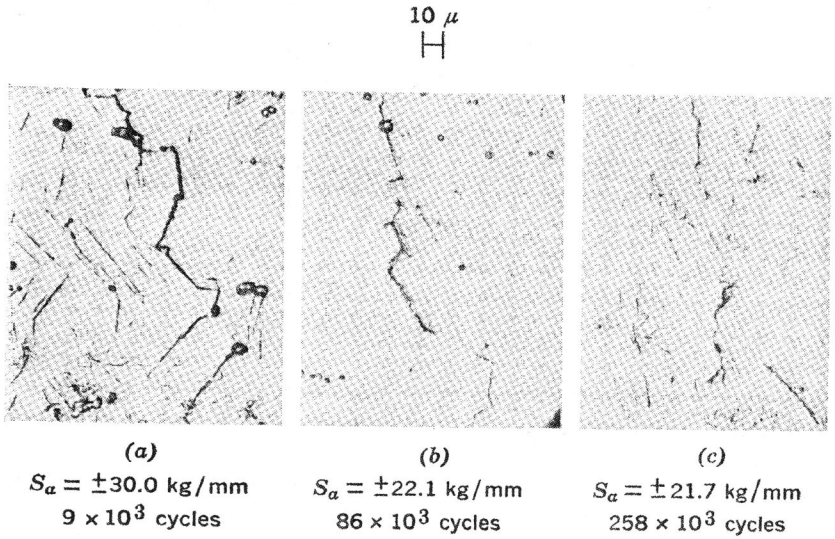

Fig. 23. Formation of slip bands and cracks in fatigued specimens of Al-Mg-Si alloy.

The chemical composition, heat-treatment, and strength values of these steels have been compiled and are presented in Table 2.

In the 17 Mn steel, which is coarse-grained, slip lines appear in many crystals after a short time of test, and they change little with increasing

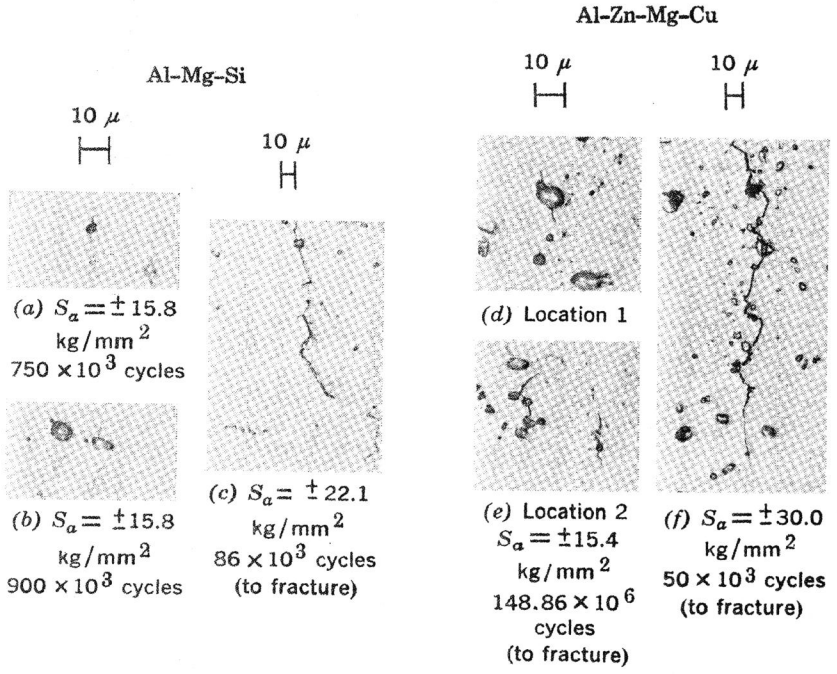

Fig. 24. Starting of cracks on inclusions in cyclically stressed specimens of Al-Mg-Si and Al-Zn-Mg-Cu alloys.

test duration. The first slip lines occur after 1000 cycles. (Even with stresses in the range of the endurance limit, as well as at higher stresses, slip lines appear at 1000 cycles, Fig. 25.) The deformation markings are characterized in this material also by single and multiple slip. The course of the fatigue cracks is determined to a particular extent by multiple slip, as can be seen from Figs. 26*b* and *c*.

In the 15 Cr-15 Ni steel, which is fine-grained, the number and extent of the slip traces also increase with increasing number of cycles, but here slip is restricted to a few crystals. It is noteworthy that, with this steel, slip takes place by preference in the form of single slip. Figure 27 shows the effect of stress level on the development of the slip lines: With decreasing stress, the number and extent of the slip lines decrease; with stresses approximately at the fatigue limit (± 22 kg/mm²), only individual slip lines develop in a few crystallites. In the same way as with the

TABLE 2. Chemical Composition, Heat-Treatment, and Strength Values of Two Austenitic Steels

	17 Mn	15 Cr-15 Ni
Chemical Composition (%)		
C	0.35	0.07
Si	—	1.02
Mn	17.2	0.72
Cr	1.5	15.8
Ni	—	15.8
Cb	—	1.05
Mo	—	2.12
N	—	0.12
Heat-Treatment	—	20 min at 1100°C, air-cooled
Stress for a Permanent Set of 0.2% (kg/mm²)	—	33.0
Ultimate Tensile Strength (kg/mm²)	78.0	68.0
Fatigue Limit * (kg/mm²)	±30.0	±22.0

* Reversed plane-bending fatigue test: $S_m = 0$, 1500 cpm, 10^7 cycles.

ferritic materials, spreading of the slip markings after initial cracking is restricted in austenitic materials to only those crystals that are situated in front of the cracks (Fig. 28). From observing individual slip bands of cyclic-stressed austenitic steel specimens in the electron microscope, it can be stated that the surfaces of these slip bands show hairline cracks (Fig. 29).

The fatigue tests carried out with body-centered and face-centered cubic materials make it evident that the formation of the slip lines depends on the stress level and test duration and that the appearance of the deformation markings, as well as the propagation of fatigue cracks, is determined by single and multiple slip. With the aluminum alloys and the austenitic steels, inclusions in the matrix, as well as the grain size of the structure, are additional factors affecting the course of slip traces and cracks.

Tests with Polycrystalline Specimens of a Body-Centered Cubic Material in Different Gas Atmospheres

The behavior of materials under fatigue stress at room temperature is determined to a particular extent by mechanical properties of the surface layer, such as roughness, grain size, strain hardening, and internal stresses.

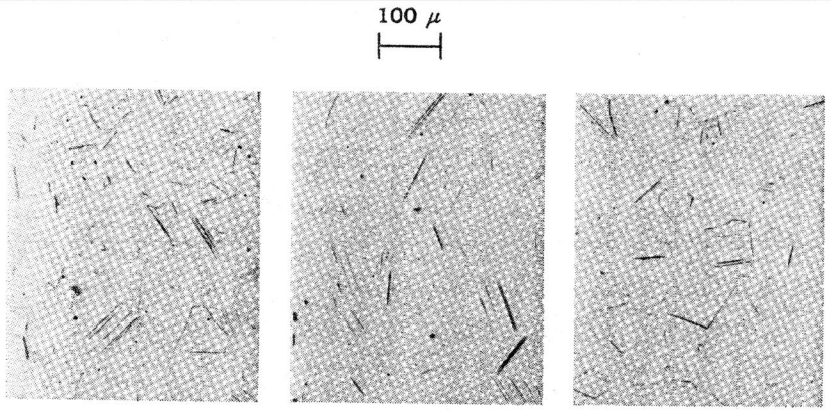

Fig. 25. Formation of slip bands in austenitic steel Type 17 Mn as related to the stress level at a constant number of cycles.

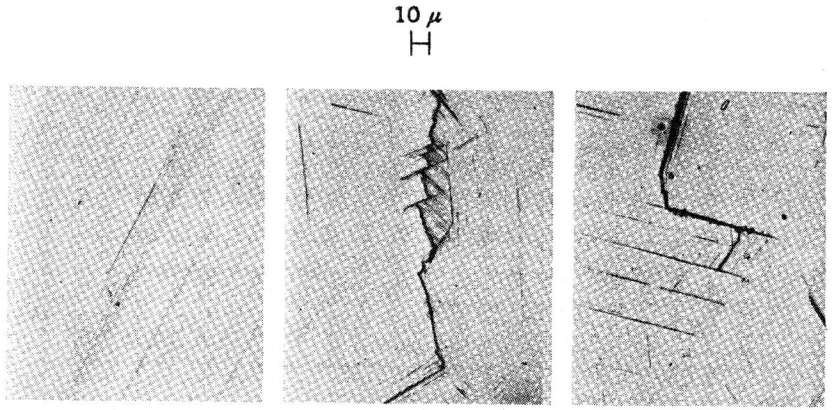

Fig. 26. Course of slip markings and cracks in austenitic steel Type 17 Mn.

As regards the magnitude of the fatigue limit, the type, humidity, pressure, and degree of purity of the ambient atmosphere are of particular importance. According to Schaub and Liedtke,[25] starting of a fatigue

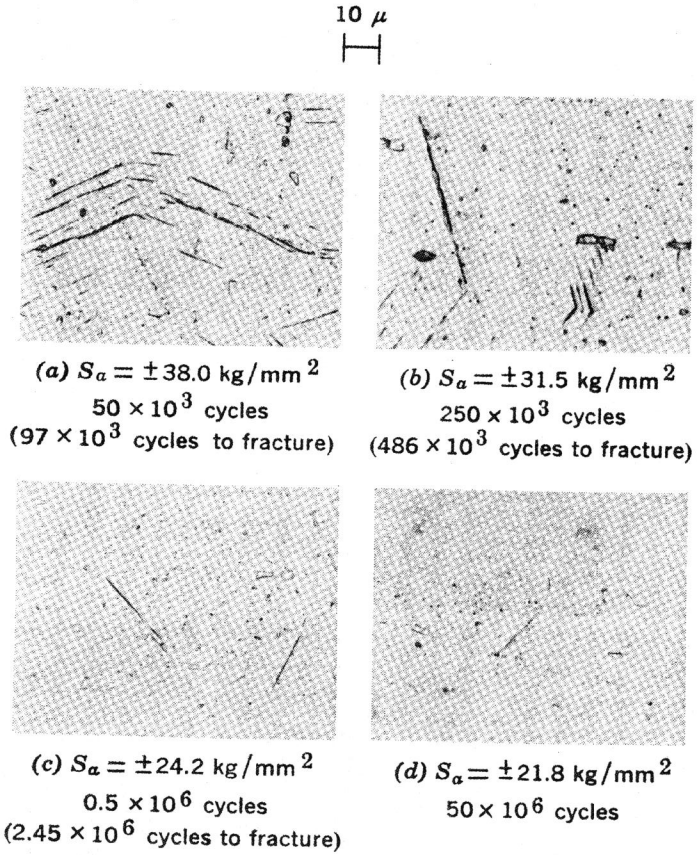

Fig. 27. Appearance of slip bands on fatigued specimens of an austenitic steel 15 Cr-15 Ni as related to the stress level.

failure at room temperature requires, aside from the occurrence of slip, reactions between the surface atoms (activated by deformation) and the surrounding atmosphere, above all with the oxygen of the air.

In order to examine the latter point, push-pull fatigue tests ($S_m = 0$, 2000 cpm) have been carried out on flat-sided round specimens of an unalloyed steel.* The specimens were washed in a special test chamber

* Steel with 0.09% C, 0.30% Si, 0.49% Mn, 0.017% P, 0.019% S, 0.004% N, and 0.016% O; annealed 1 hr at 930°C and air-cooled. Upper/lower yield strength = 28.4/25.1 kg/mm²; ultimate tensile strength = 40.8 kg/mm².

by such purified and dried gases as O_2, N_2, H_2, and Ar. In addition, corresponding tests have been carried out in laboratory air.[16] Figure 30 represents the S–N diagram of the different series of experiments. According to these tests, the various gases affect neither the lifetime nor the fatigue limit of this steel. With a scatter range of ±1 kg/mm², the

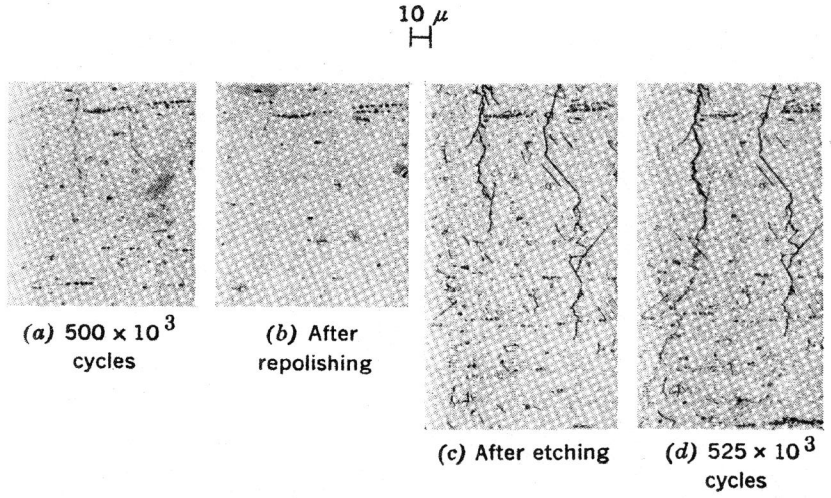

Fig. 28. Propagation of slip traces and cracks in fatigued steel specimens 15 Cr-15 Ni. $S_a = \pm 28.0$ kg/mm², 0.61 × 10^6 cycles to fracture.

fatigue limit is ±18.0 kg/mm². In Fig. 31, some of the test results on the deformation markings in different atmospheres are given for several stress amplitudes. The starting, propagation, and appearance of the slip traces do not depend on the gas atmosphere.

In the steel investigated, therefore, neither the fatigue limit nor the formation of slip markings is affected by the presence of a reactive gas atmosphere. It may be concluded that general application of the hypothesis of Schaub and Liedtke [25] to all metallic materials will not be possible.

Tests at Low Temperatures

With alternating stress at low temperatures, a higher stress is required to create a critical state at energetically favored places of the lattice owing to the more intensive heat emission. This higher stress enables atoms to move, and, in connection therewith, slip or yielding to take place. From earlier studies on mechanical twins, it can be concluded that the threshold energy at which formation of twins sets in will be de-

pendent on several factors, particularly on the type and state of the material, the speed of deformation, the stress level, the test temperature, and the state of stress.[26,27]

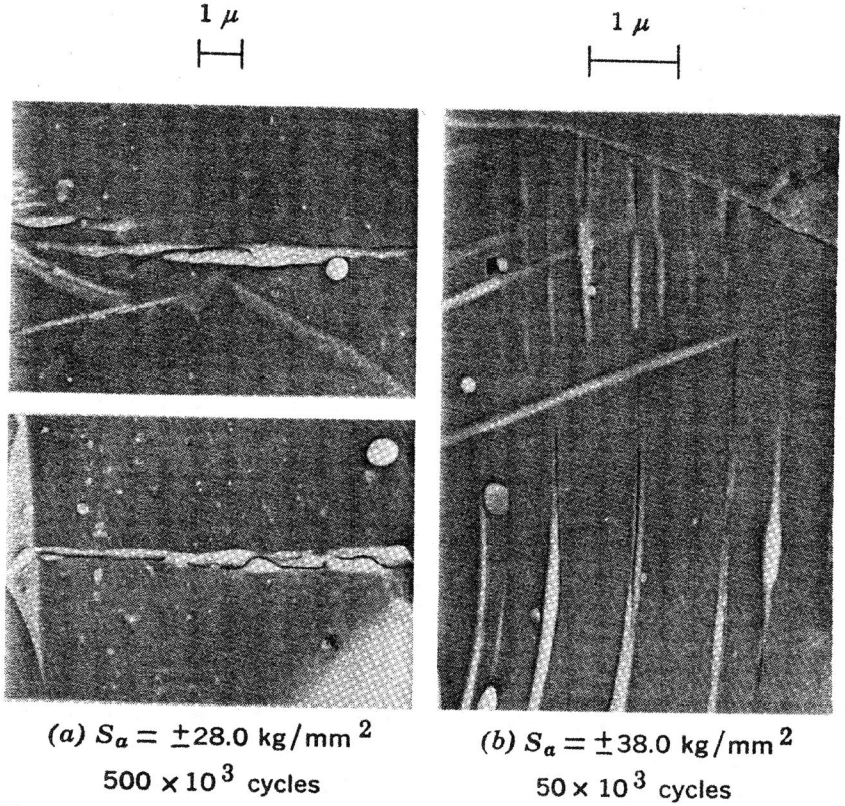

Fig. 29. Electron micrographs (plastic replica) of slip bands of fatigued specimens of the steel Type 15 Cr-15 Ni.

In order to complete the observations on the changes in structure found at room temperature, the effect of a test temperature of −180°C (liquid air) on the deformation phenomena of unnotched, flat-sided round bars of an Armco iron* has been determined in push-pull fatigue tests ($S_m = 0$, 2000 cpm).[16] (For the metallographic studies, the surfaces of the specimens were electrolytically polished.) As an example, Fig. 32 shows the shape of deformation traces at −180°C with a stress amplitude of

* Armco iron with 0.036% C, 0.07% Si, 0.08% Mn, 0.021% P, 0.011% S, and 0.03% O; annealed 1 hr at 930°C and air-cooled. Upper/lower yield strength = 28.1/22.3 kg/mm², ultimate tensile strength = 34.0 kg/mm².

±52 kg/mm² as dependent on the number of cycles. Under these test conditions, the deformation is characterized not by slip lines but by the formation of twins. That the traces are really twins is confirmed by the photographs in Fig. 33. The outstanding features of twins are distinctly evident: They appear in the different ferrite grains as narrow bands that mostly run from one grain boundary to the other. In addition, the

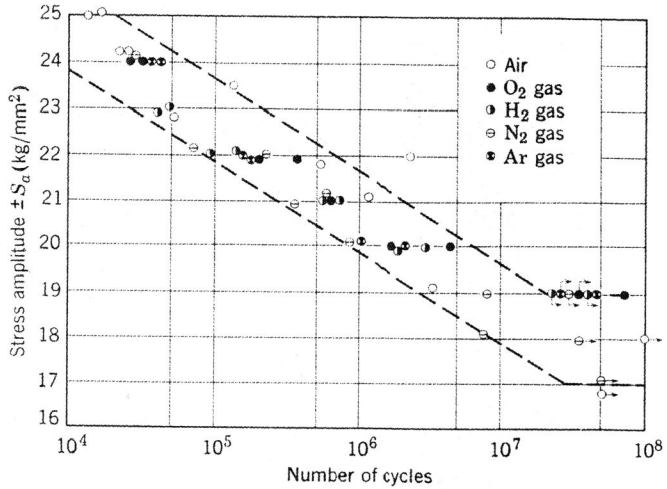

Fig. 30. *S–N* diagram for push-pull tests of flat-sided round specimens of an unalloyed 0.09% C steel in different gas atmospheres. $S_m = 0$, 2000 cpm.

single twinning bands frequently show splits and interruptions. With the specimens stressed above the fatigue limit, these twins can be observed in many crystallites, whereas they are absent in the specimens stressed in the range of the fatigue limit. These findings indicate that, for the formation of twins under cyclic stress and at low temperature, a barrier of deformation or energy must be crossed. The particular feature in this case is that, to start the formation of twins, a strain rate in the fatigue test of about 20 to 40%/sec suffices.

In order to examine whether and in what manner slip markings observed at room temperature are affected by an alternating stress at low temperature, the following tests were carried out: Some specimens were prestressed either at 20° or −180°C until deformation traces showed up, and then they were loaded further at a temperature of −180° or 20°C with a corresponding stress amplitude. Results of such a series of tests are presented in Fig. 34. At the temperature of prestressing, only one type of deformation occurs. The additional occurrence of twins or slip

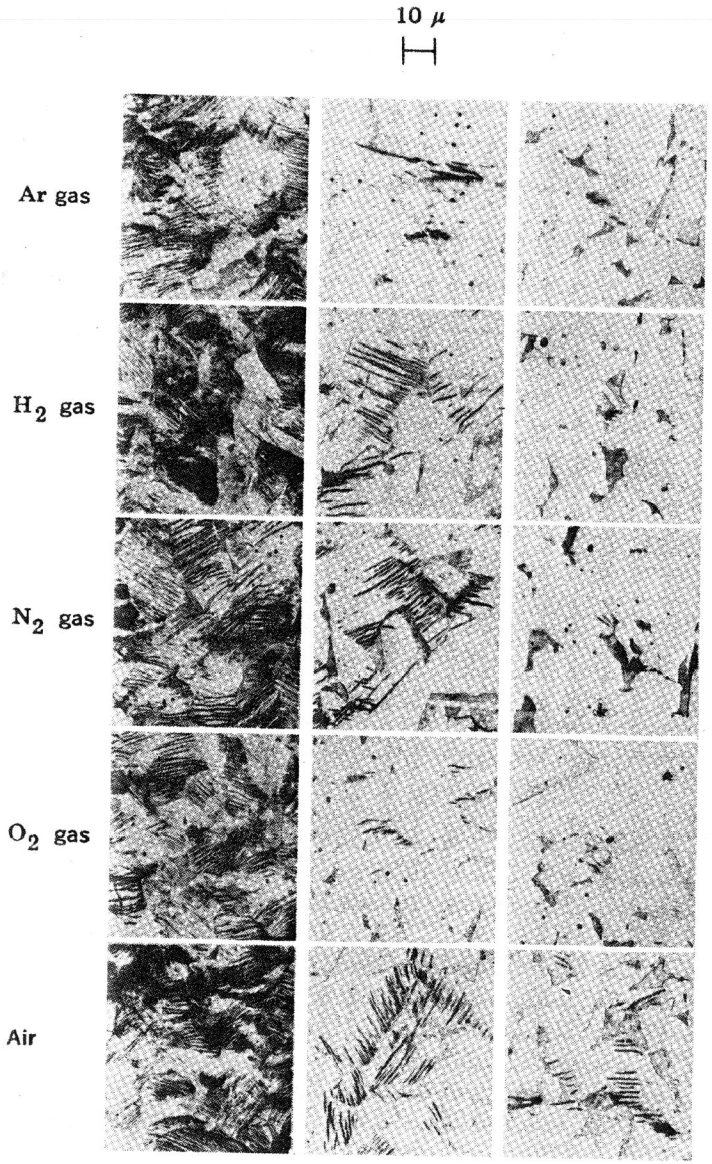

Fig. 31. Formation of slip bands in flat-sided round specimens of 0.09% C steel at several stress amplitudes in different gas atmospheres. Push-pull fatigue test. $S_m = 0$, 2000 cpm.

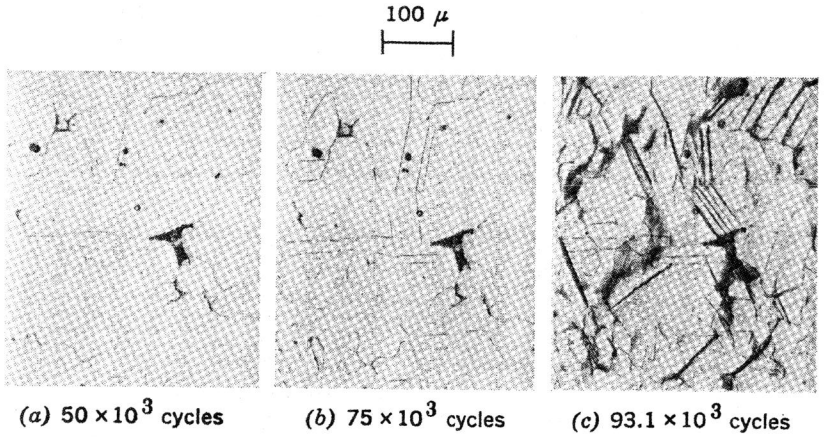

Fig. 32. Formation of twins in cyclically stressed specimens of Armco iron at −180°C as related to number of cycles. Push-pull fatigue test. $S_m = 0$, 2000 cpm; $S_a = \pm 52.0$ kg/mm². 93.1 × 10³ cycles to fracture.

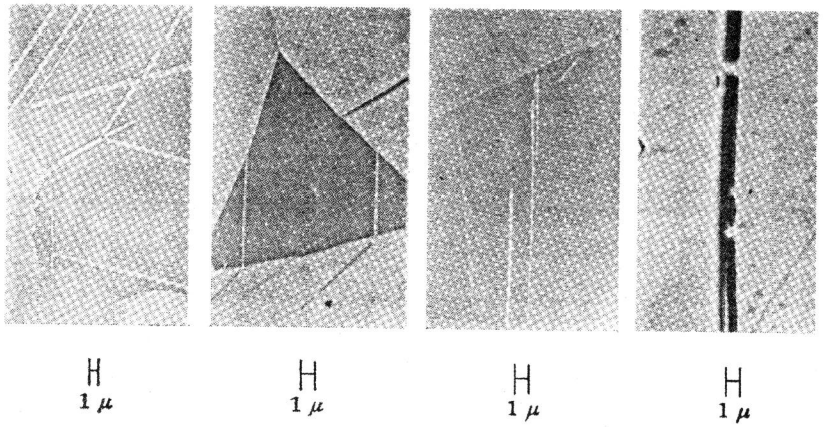

Fig. 33. Signs of twins at higher magnification. $S_a = \pm 55.8$ kg/mm², 0.306 × 10⁶ cycles to fracture.

markings with subsequent testing indicates that both of the deformation phenomena are taking place independently and that they are both stable.

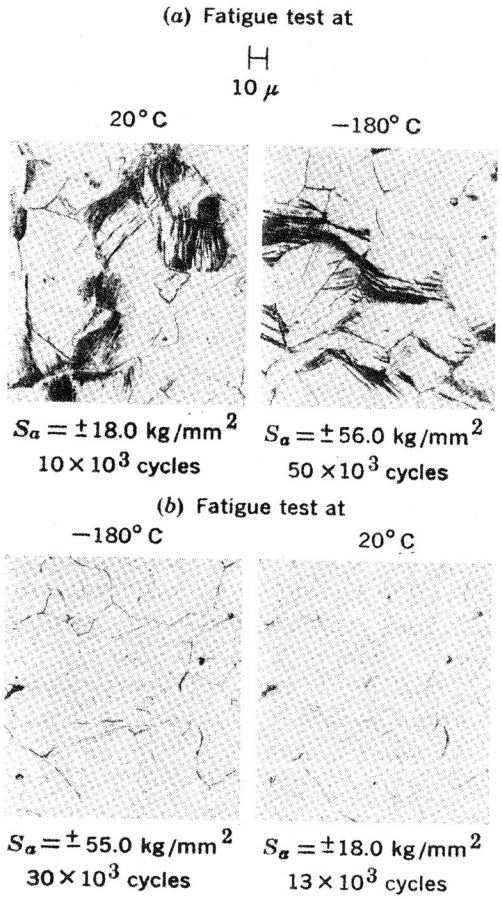

Fig. 34. Deformation traces in cyclically stressed specimens. (*a*) Tested first at 20°C for 10×10^3 cycles, then tested at −180°C for 50×10^3 cycles. (*b*) Tested first at 180°C for 30×10^3 cycles, then tested at 20°C for 13×10^3 cycles.

Tests at High Temperatures

In order to determine the processes taking place in heat-resisting materials at high temperatures under static and cyclic stress, carbide isolation tests, as well as metallographic studies, have been carried out with good results. The residues recovered from these isolation tests were

analyzed microchemically in order to determine the proportions of the various alloying elements. From the Debye-Scherrer diagrams of the residues, data can be gathered on the different types of crystals isolated.[28–30]

In Fig. 35, some of the results of the metallographic investigations of

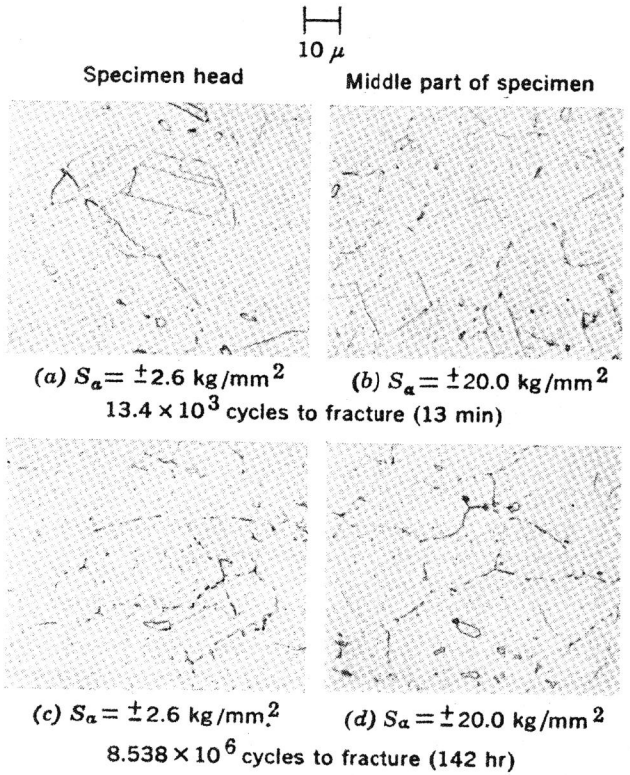

Fig. 35. Structural changes of fatigued specimens of steel 15 Cr-15 Ni tested at 650°C. Push-pull fatigue test. $S_m = 0$, 1000 cpm.

specimens of an austenitic steel (15 Cr-15 Ni) are presented. The specimens have been tested at 650°C by push-pull ($S_m = 0$, 1000 cpm).[31] For purposes of comparison, micrographs of sections taken from the test bar head are shown against those taken from the test section. At the same stress amplitude, these specimens gave different times to fracture. The reason for this is the difference of the structure. One specimen is fine-grained and the other shows a mixed fine- and coarse-grained structure. In the coarse-grained specimen, which fractured after 13,400 cycles (13 min), only small precipitation, if any, occurs now and then

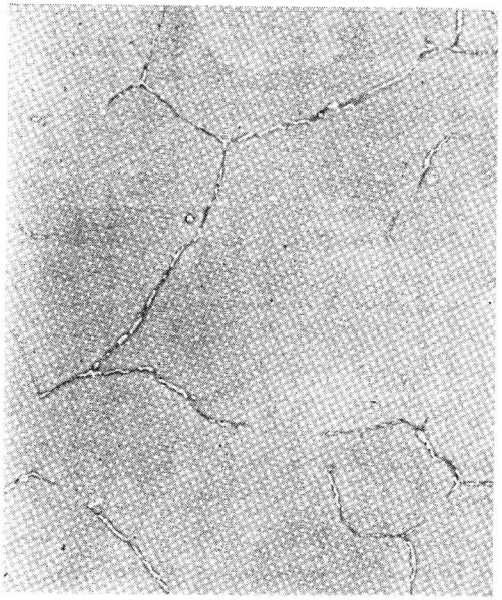

Fig. 36. Electron micrograph (plastic replica) of carbide precipitation on grain boundaries of an austenitic steel 15 Cr-15 Ni tested at 650°C. $S_a = \pm 20.0$ kg/mm², 8.538×10^6 cycles to fracture.

at the grain boundaries. In the fine-grained specimen, stressed for 8.538×10^6 cycles (142 hr), fine precipitates of carbide on the grain boundaries can be distinctly seen. The precipitates also occur in the head of the specimen, which has been stressed at only 2.6 kg/mm². It may be concluded that long annealing without an external load will lead to similar changes of structure. This conclusion is fully confirmed by the data obtained in long-time creep tests from the heads and test sections of austenitic steel specimens.[28–30] Of particular clarity are the changes in structure seen when the specimens are observed under the electron microscope (Fig. 36). The grain boundaries are etched deeper than the grains; they are, therefore, darker and filled with carbide precipitates (bright grains).

In accordance with the changes observed in the microstructure of cyclic-stressed specimens of this steel, there are also alterations that can be seen from X-ray and microanalysis of the isolated residues. Table 3 gives the data of the microchemical analysis of three specimens of the type 15 Cr-15 Ni steel.

TABLE 3. Microchemical Analysis of Type 15 Cr-15 Ni Steel

Specimen No.	Testing Temperature (°C)	Stress Level (kg/mm²)	Lifetime	Content (%) Fe	Cr	(Cb + Ta)
1	—	—	—	6.7	19.2	64.0
2	600	±24.0	4 min	7.0	19.4	63.5
3	600	±22.0	53.5 hr	24.6	32.2	24.4

While the microanalyses of the residues from the unstressed specimen and the specimen stressed 4 min yield evidence of the same composition, the specimen stressed 53.5 hr shows strong concentrations of Fe and Cr and a decrease in the content of (Cb + Ta). X-ray analysis yields evidence in all three cases of the carbide (Cb, Ta) C and γ-Fe. The increase in the values of Fe and Cr in the microanalysis thereby indicates an increase of the amount of γ-iron with increasing time of stress.

If one considers as a whole the structural changes at high temperatures caused by different conditions of stress (long-time annealing without load, static or cyclic loading), it can be stated that the extent of these changes, but not their type, depends on these conditions. By holding at elevated temperature alone, without the action of an external stress, the structural changes occur only after a very long time. The addition of deformation by a constant tension stress leads to a shortening of the test duration required. Cyclic strains under fatigue stress accelerate the occurrence of the structural changes still more.

Summary

The number and extent of slip traces in all the materials tested (carbon steels, α-iron single crystals, pure aluminum, aluminum alloys, and austenitic steels) are affected by the stress amplitude and the test duration. The occurrence of the first slip lines with decreasing stress is displaced to higher numbers of cycles. Slip lines occur in some materials (carbon steel, pure aluminum, austenitic steel 17 Mn) with stresses below the fatigue limit, whereas in other materials (aluminum alloys, α-iron single crystals, austenitic steel 15 Cr-15 Ni) slip markings occur only with stresses at and above the fatigue limit.

The appearance of the slip traces and the course of the fatigue cracks in single-crystal and polycrystalline materials are determined by the processes of single and multiple slip in crystals of different orientation. In aluminum alloys and the 15 Cr-15 Ni austenitic steel, microstructure also plays an important part.

At the surface of the slip bands of unalloyed, austenitic steels and α-iron single crystals, minute cracks occur; deep cavities and grooves occur in the case of pure aluminum. All these favor the formation of microcracks and macrocracks.

Different gas atmospheres do not affect the fatigue behavior of an unalloyed steel at room temperature. Furthermore, there is no effect by the different gases on the formation and appearance of slip traces on the specimens.

Twins form in Armco iron fatigue specimens tested at a temperature of -180°C and at stresses approximately equal to the fatigue limit or higher. The strain rate in the fatigue test (20 to 40%/sec) initiates this formation of twins.

The specimens of a 15 Cr-15 Ni austenitic steel tested at temperatures of 600° and 650°C show carbide precipitation on the grain boundaries. The precipitation is greatly accelerated by fatigue stressing.

REFERENCES

1. H. J. French, *Trans. Amer. Soc. Steel Treating*, **21,** 899 (1933).
2. U. Dehlinger, *Z. Physik*, **115,** 625 (1940).
3. A. Kochendörfer, *Plastische Eigenschaften von Kristallen und metallischen Werkstoffen*, J. Springer, Berlin, p. 253 (1941).
4. E. S. Machlin, "Dislocation Theory of the Fatigue of Metals," *Nat. Advisory Comm. Aeronaut. Tech. Note No.* 1489 (1948).
5. J. A. Ewing and J. W. C. Humfrey, *Phil. Trans. Roy. Soc. (London), A,* **200,** 241 (1903).
6. H. J. Gough, *Proc. Amer. Soc. Testing Materials*, **33,** 3 (1933).
7. H. F. Moore and T. Ver, "A Study of Slip Lines, Strain Lines and Cracks in Metals under Repeated Stress," *Univ. Illinois Engng. Exp. Stat. Bull. No.* 208 (1930).
8. A. Kochendörfer, *Z. Elektrochem.*, **56,** 283 (1952).
9. A. Kochendörfer, *Physik. Bl.*, **7,** 151, 252, and 502 (1951).
10. A. Kochendörfer, *Z. Ver. deut. Ingr.*, **94,** 267 (1952).
11. N. F. Mott, *Proc. Roy. Soc. (London), A,* **242,** 145 (1957).
12. N. Thompson and N. J. Wadsworth, *Phil. Mag. Suppl.*, **7,** 72 (1958).
13. M. Hempel, *Colloquium on Fatigue*, J. Springer, Berlin, p. 78 (1956).
14. F. Wever, M. Hempel, and A. Schrader, *Arch. Eisenhüttenw.*, **26,** 739 (1955).
15. M. Hempel, *Proceedings International Conference on Fatigue of Metals*, Institution of Mechanical Engineers, London, p. 543 (1957).
16. Unpublished data of the Max Planck Institute, Düsseldorf, to be in *Arch. Eisenhüttenw.*
17. N. E. Frost and C. E. Phillips, *Proceedings International Conference on Fatigue of Metals*, Institution of Mechanical Engineers, London, p. 520 (1957).
18. M. Hempel, A. Kochendörfer, and E. Hillnhagen, *Arch. Eisenhüttenw.*, **28,** 417 (1957).
19. M. Hempel, A. Kochendörfer, and E. Hillnhagen, *Arch. Eisenhüttenw.*, **28,** 433 (1957).

20. M. Hempel and E. Hillnhagen, *Rev. mét.*, **55,** 749 (1958).
21. N. P. Allen, B. E. Hopkins, and Y. E. McLennan, *Proc. Roy. Soc. (London), A,* **234,** 221 (1956).
22. M. Hempel and A. Schrader, *Arch. Eisenhüttenw.*, **28,** 547 (1957).
23. A. Kochendörfer, *Arch. Eisenhüttenw.*, **25,** 351 (1954).
24. S. Mader, *Z. Physik*, **149,** 73 (1957).
25. C. Schaub and W. Liedtke, *Colloquium on Fatigue*, J. Springer, Berlin, p. 244 (1956).
26. H. Hanemann and A. Schrader, *Atlas Metallographicus*, Vol. 1, Gebr. Borntraeger, Berlin, p. 57 and Tables 83 and 84 (1933).
27. R. Clark and G. B. Craig, *Progress in Metal Physics*, Vol. 3, B. Chalmers, Ed., Pergamon Press, London, p. 115 (1952).
28. A. Krisch, *Arch. Eisenhüttenw.*, **28,** 305 (1957).
29. F. Wever, A. Krisch, and H. J. Wiester, *Arch. Eisenhüttenw.*, **26,** 463 (1955).
30. F. Wever and A. Schrader, *Arch. Eisenhüttenw.*, **26,** 475 (1955).
31. F. Wever and M. Hempel, *Forschungsberichte des Wirtschafts- und Verkehrsministeriums Nordrhein-Westfalen*, No. 312 (1956).

DISCUSSION

A. Johansson, *STAL Turbine Co., Sweden.* It would be of interest to determine if the carbide precipitation observed by Hempel at the grain boundaries of 15 Cr-15 Ni sheet tested in fatigue at 600° and 650°C has any influence on the formation of the cracks and the fatigue mechanism. Similar observations have been made during fatigue tests of 18-8 Cr-Ni sheet at 500°C.[1] Cylindrical test pieces were exposed to alternating bending over a fixed diameter. After about 1000 cycles, a section through the test piece showed no change in the structure near the neutral axis, but carbide precipitation was clearly visible where the strain amplitude had been ± 0.1 to ± 0.2%. The precipitation increased with the distance from the neutral axis.

However, there was no tendency at all for the fatigue cracks to follow the grain boundaries, or, as far as could be determined, to be even influenced by the position of the grain boundaries. The number of strain cycles for fracture at a given strain amplitude was about the same at room temperature, at 300°C, and at 500°C. At the lower temperature, there was no evidence of carbide precipitation. It is therefore difficult to imagine that in these tests the carbide precipitation has anything to do with the formation or development of the fatigue cracks. As also pointed out by Hempel, it is only the normal carbide precipitation in these sheets at high temperatures that is greatly accelerated by the plastic deformation.

Reference

1. A. Johansson, *Proceedings of the Colloquium on Fatigue*, I.U.T.A.M. Colloquium, Stockholm, 1955, Springer-Verlag, Berlin, p. 112 (1956).